POS Assisted Aerial Triangulation Method for Single Flight Strip Without Ground Control Points

Jianchen Liu, Rumeng Li, and Wei Guo

***Abstract*—In scenarios such as road detection and emergency mapping, single strip photogrammetry without ground control points (GCPs) can effectively improve data acquisition efficiency. Positioning and orientation system (POS) assisted single strip aerial triangulation utilizes relative orientation to construct a strip model. However, due to factors such as cumulative errors, the strip model can experience distortion. The distortion affects the accuracy of aerial triangulation solutions and can even render the results unavailable. In addition, the attitude data from POS may not be precise enough, especially the yaw angle. To address this issue, this article proposes a POS assisted aerial triangulation method for single flight strip without GCPs. This method establishes an error correction model. By utilizing the exterior orientation elements observed by the POS system, this method corrects the less accurate position and attitude parameters obtained after relative orientation. This correction process results in obtaining high precision exterior orientation elements for the images. Moreover, the error correction model maintains a constant number of parameters, regardless of the quantity of images, with only 18 parameters, thus ensuring efficient model solving. Ultimately, through experimental validation, it has been demonstrated that the method proposed in this article has improved the overall accuracy by approximately 13.22% and 17.72% compared to traditional POS assisted bundle adjustment methods under different flight strips and varying attitude angle errors, separately.**

***Index Terms*—Aerial triangulation, positioning and orientation system (POS) assisted, single flight strip, without ground control point (GCP).**

I. Introduction

THE advancement of photogrammetry technology has raised higher demands for efficiency and accuracy in three-dimensional (3-D) modeling, particularly in fields of emergency rescue and mobile surveying [1], [2]. In the traditional pipeline of 3-D reconstruction, multistrip data can provide forward overlap information and lateral overlap information. However, in the case of elongated and narrow terrains, such as railways, highways, rivers, or specific scenarios such as pavement distress detection and emergency mapping, the acquired single strip image data provide only forward overlap information [3].

Manuscript received 11 October 2023; revised 20 December 2023; accepted 22 February 2024. Date of publication 29 February 2024; date of current version 14 March 2024. This work was supported in part by the National Natural Science Foundation of China under Grant 42171439 and in part by the Qingdao Science and Technology Demonstration and Guidance Project under Grant 22-3-7-cspz-1-nsh. *(Corresponding author: Wei Guo.)*

The authors are with the College of Geodesy and Geomatics, Shandong University of Science and Technology, Qingdao 266590, China (e-mail: liujianchen@sdust.edu.cn; lirumeng98@163.com; 17685542660@163.com).

Digital Object Identifier 10.1109/JSTARS.2024.3371423

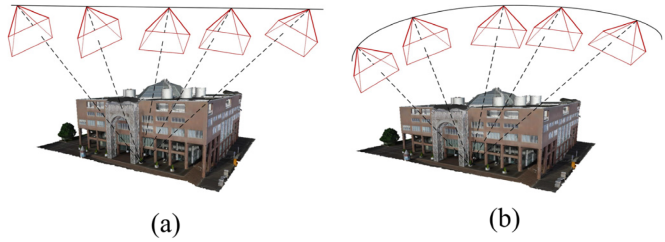

Fig. 1. Comparison of POS Observational strip model with relative orientation strip model. (a) POS observational. (b) Relative orientation.

Furthermore, the construction of the flight strip model relies on dependent relative orientation, a crucial step in photogrammetry [4], [5]. Its objective is to determine the relative position and orientation between neighboring images [6], this can directly affect the quality and accuracy of subsequent mapping tasks [7]. However, due to the process of relative orientation, errors often accumulate with the increasing number of images within the strip. This ultimately results in the deformation of the strip model and the low accuracy of the solved image external orientation (EO) element. As shown in Fig. 1, (a) represents the strip model obtained through aerial triangulation assisted by the navigation positioning and orientation system (POS) and (b) represents the strip model obtained through relative and absolute orientation. It is evident that strip (b) exhibits significant deformation compared to strip (a), indicating lower image EO accuracy achieved through relative orientation. Therefore, in the case of single strip, how to eliminate the deformation of the flight strip due to the accumulation errors in the relative orientation, and improve the stability of the flight strip model and the accuracy of the solution are the difficulties content of the present research.

As the global navigation satellite system (GNSS) and inertial measurement unit (IMU) continue to advance [8], the utilization of POS assisted aerial triangulation has the potential to reduce the necessity for ground control points (GCPs) and improve efficiency [9], [10]. In addition, the outcomes of aerial triangulation without GCPs can generally meet the accuracy demands of most photogrammetric products [11], [12]. However, due to the cost constraints associated with IMU or inherent yaw angle system errors [13], attitude data often lacks the necessary precision. In such instances, single strip aerial triangulation may be confronted several issues. First, using POS data as the initial values for bundle adjustment (BA) can significantly impact the accuracy of aerial triangulation [14]. Although it is possible to directly weight image exterior orientation (EO) during the solution process, this approach has its drawbacks. When given

weights are excessively large, the EO correction value becomes very small. In such cases, if the initial value lacks sufficient accuracy, it directly affects the accuracy of the BA solution and may even lead to a failure. Conversely, when given weights are too small, obtaining accurate results also becomes challenging. Second, utilizing the outcomes of relative orientation as the initial values for BA, the cumulative errors from relative orientation can result in the deformation of the constructed strip model, causing the accuracy of the solution results to fall short of practical application requirements.

To address the aforementioned problems, this article introduces a POS assisted single strip aerial triangulation method without GCPs that considers the accumulation error in relative orientation. This method builds upon traditional techniques by correcting the cumulative error in relative orientation. While POS can provide precise positional information, accurate relative attitude information can be acquired through relative orientation. Therefore, the approach presented in this article aims to leverage the strengths of these two methods to achieve highly accurate image EO. This method can mitigate flight strip curvature and improve geometric accuracy by employing POS data to assist single strip aerial triangulation. An error correction model is established by combining the POS data with the relative orientation, which accounts for the cumulative error in relative orientation. In contrast to the mathematical model of traditional BA, the number of unknowns in this method is independent of the number of images. As a result, the size of the normal equation coefficient matrix is significantly reduced.

The rest of this article is structured as follows: In Section II, this article discuss existing POS assisted single strip aerial triangulation methods and relative orientation. Section III describes the proposed method and its key steps in detail. In Section IV, this article conducts several experiments to verify the effectiveness of the method and evaluate its performance. Finally, Section V concludes this article.

II. Related Work

At present, aerial triangulation methods are mainly summarized into three types: the direct georeferencing (DG) method; relative and absolute orientation method; and POS assisted BA method [15]. The DG method uses the airborne GNSS and the IMU to acquire the EO elements of the images [16]. The relative and absolute orientation method obtains the EO elements of the images by solving the coplanarity conditional equations. The POS assisted BA method uses only the POS data and tie points to compute the EO elements of the images. The method proposed in this article is related to the relative and absolute orientation method and the traditional POS assisted aerial triangulation method.

Relative orientation is one of the most important steps in the field of photogrammetry [17]. Currently, the widely used relative orientation methods can be divided into two steps. The first step involves determining the values of the essential matrix elements by solving a linear system of equations using sufficient corresponding feature points. The second step involves a non-linear method to recover the relative orientation parameters (i.e., three translation parameters and the rotation matrix) from the essential matrix. The essential matrix solved by linear methods with eight corresponding points was first introduced by Longuet Higgins [18]. Subsequently, Nister [19] proposed an effective five point method for solving the essential matrix. However, in the case of purely rotational motion, the essential matrix approach to estimating the relative orientation parameters is inadequate [20]. As an alternative, methods that do not use the essential matrix have been proposed by Kneip and Lynen [21], which either estimate the relative attitude using quaternionsor make use of the epipolar constraint. However, in the absence of auxiliary data, the relative orientation of a single strip can easily cause the bending deformation [22] due to accumulated errors.

The POS system can obtain the real-time imaging positions and attitudes from sensors, and have been widely used in POS assisted BA methods. The more accurate EO elements of the image can be obtained through BA without GCPs. This has promoted the development of UAV photogrammetry in reducing the number of GCPs or not setting up GCPs. To solve the problem of bending deformation in flight strip, a lot of work has been carried out on POS assisted aerial triangulation. He et al. [23] proposed a framework for automated aerial triangulation for UAV photography. This framework can be superior in providing 3-D models when using UAV images that contain repeating patterns and significant image distortions. Turner et al. [24] showed the results of processing high resolution UAV images using PhotoScan and Pix4D softwares, and an Bundler method without GCPs. Tanathong and Lee [25] used GPS/INS data to improve the accuracy and speed of aerial triangulation. Wierzbicki [26] introduced displacement deviation error measurements to aerial triangulation. Choi and Lee [27] proposed an incremental aerial triangulation method that produces accurate results in real time using traditional aerial triangulation Further, Forlani et al. [28] presented a ground photogrammetry method without utilizing GCPs. The on the job camera self-calibration using BA method also has a significant impact on accuracy [29]. Due to the cost constraints of IMU and their inherent systematic errors, accurate initial values are usually not available before the BA process.

The development of photogrammetric technology is very rapid, and various methods have been proposed to process specific data. But there are fewer researches on POS assisted single strip aerial triangulation. To address the above issues, this article seeks to obtain an accurate result of the flight strip model by developing an error correction model, and this article combines the advantages of the relative orientation and the POS assisted aerial triangulation method. The error correction model in this article is constructed based on the polynomial model, which has the advantages of simplicity, efficiency, and reducing the number of unknowns.

III. Methodology

A. Overview of Proposed Approach

The method proposed in the article combines POS data with relative orientation results to build a single strip error correction model. This method effectively addresses the issue of error accumulation. Furthermore, this method not only reduces the number

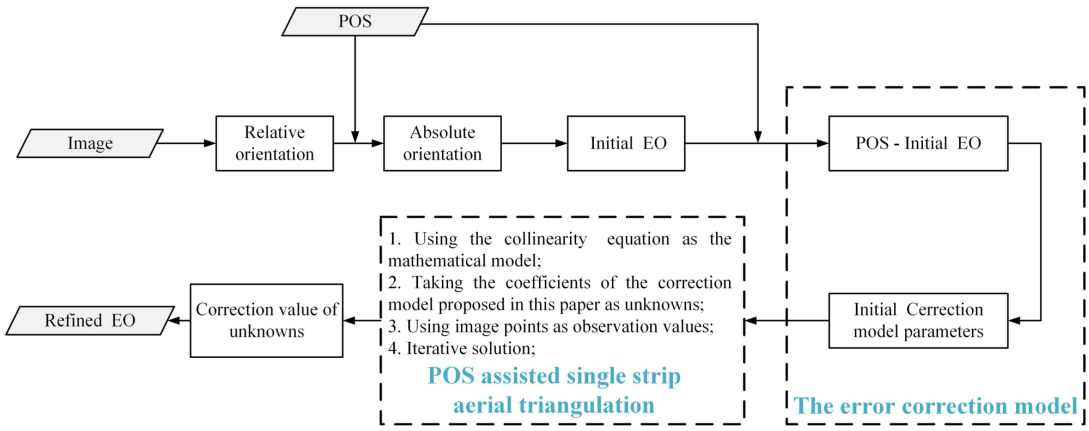

Fig. 2. Overall workflow of the proposed approach.

of parameters, thereby improving computational efficiency, but also demonstrates significantly improvement compared to traditional methods. The technical pipeline of the POS assisted aerial triangulation method for a single strip without GCPs is illustrated in the Fig. 2.

First, relative orientation is performed. To unify the coordinate system, the POS data is used for absolute orientation to obtain the initial image EO. The cumulative error of relative orientation is related to the number of the images, it increases with the distance between the current image and the reference image. Therefore, this method establishes the error correction model of the image EO for a single strip, and the initial values of the parameters in the error correction model are fitted according to the POS data and the initial image EO. Then, the collinearity equations were constructed for POS assisted single strip BA, where the image point coordinates are observations, the 18 parameters of the error correction model and the object point coordinates are unknowns. Finally, the optimal coefficients of the error correction model are obtained, so that the accuracy of the image EO is improved.

B. Single Strip BA Model Considering Cumulative Errors

For single flight strip, with the first image as the reference, the farther away from the first image, the larger the cumulative error of the image EO will be. Therefore, in this article, from the mechanism of relative orientation cumulative error, the proposed method constructs the POS assisted single strip BA model with consideration of the relative orientation cumulative error. This model can eliminate the influence of relative orientation cumulative error in the BA process, and improve the solving accuracy of the POS assisted single strip BA. The error correction model is as follows:

$$\begin{aligned}
\Delta X_t &= X_0 + X_1 t + X_2 t^2 \\
\Delta Y_t &= Y_0 + Y_1 t + Y_2 t^2 \\
\Delta Z_t &= Z_0 + Z_1 t + Z_2 t^2 \\
\Delta yaw_t &= yaw_0 + yaw_1 t + yaw_2 t^2 \\
\Delta pitch_t &= pitch_0 + pitch_1 t + pitch_2 t^2 \\
\Delta roll_t &= roll_0 + roll_1 t + roll_2 t^2
\end{aligned} \tag{1}$$

where $X_0, X_1, X_2 \ldots .\mathrm{roll}_0, \mathrm{roll}_1, \mathrm{roll}_2$ represent 18 parameters in the error correction model; t indicates the distance from the reference image; and $\Delta X, \Delta Y, \Delta Z, \Delta\mathrm{yaw}, \Delta\mathrm{pitch}, \Delta\mathrm{roll}$ represent the error corrections of EO.

The process of solving the error correction model is similar to the basic principle of traditional BA, and its mathematical model relies on collinearity equations. It establishes the collinear relationship among three elements: the projection center, the image point, and the object point. The general equation of the collinearity condition is as follows:

$$\begin{aligned}
x - x_0 = F_1 &= -f\frac{U}{W} = -f\frac{a_1(X-X_s)+b_1(Y-Y_s)+c_1(Z-Z_s)}{a_3(X-X_s)+b_3(Y-Y_s)+c_3(Z-Z_s)} \\
y - y_0 = F_2 &= -f\frac{V}{W} = -f\frac{a_2(X-X_s)+b_2(Y-Y_s)+c_2(Z-Z_s)}{a_3(X-X_s)+b_3(Y-Y_s)+c_3(Z-Z_s)}.
\end{aligned} \tag{2}$$

In the equation, *(x, y)* denotes the coordinates of the image point, *(x_0, y_0)* denotes the coordinates of the image principal point, *f* represents the focal length, *(X, Y, Z)* denotes the coordinates of the ground point, *(Xs, Ys, Zs)* denotes the coordinates of the center point of the photography, and a_i, b_i, c_i (i = 1,2,3) are the elements of the 3 × 3 rotation matrix *R* generated from the three attitude elements in the image EO.

According to parameters of the corresponding error correction model, the new image EO can be obtained by adding the corrections. This is shown in the following equation:

$$\begin{aligned}
X_s &= X_{\mathrm{rel}} + \Delta X_t \\
Y_s &= Y_{\mathrm{rel}} + \Delta Y_t \\
Z_s &= Z_{\mathrm{rel}} + \Delta Z_t \\
\mathrm{yaw}_s &= \mathrm{yaw}_{\mathrm{rel}} + \Delta\mathrm{yaw}_t \\
pitch_s &= \mathrm{pitch}_{\mathrm{rel}} + \Delta\mathrm{pitch}_t \\
\mathrm{roll}_s &= \mathrm{roll}_{\mathrm{rel}} + \Delta\mathrm{roll}_t
\end{aligned} \tag{3}$$

where $X_s, Y_s, Z_s, \mathrm{yaw}_s, \mathrm{pitch}_s, \mathrm{roll}_s$ denote the new image EO obtained by the error correction model and $X_{\mathrm{rel}}, Y_{\mathrm{rel}}, Z_{\mathrm{rel}}, \mathrm{yaw}_{\mathrm{rel}}, \mathrm{pitch}_{\mathrm{rel}}, \mathrm{roll}_{\mathrm{rel}}$ denote the initial image EO.

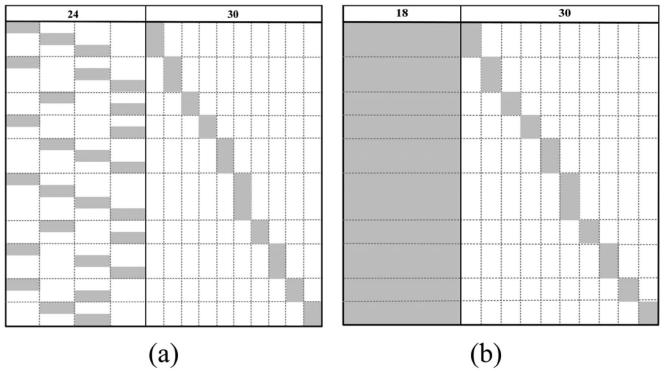

Fig. 3. Structure diagram of the coefficient matrix of the error equation. (a) Traditional aerial triangulation method. (b) Processed method.

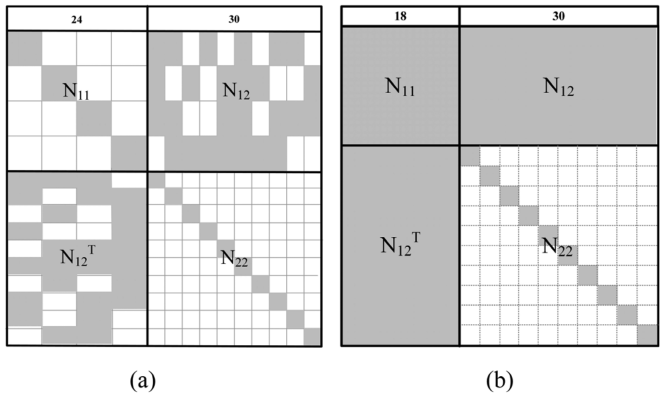

Fig. 4. Structure diagram of the coefficient matrix of the normal equation. (a) Traditional aerial triangulation method. (b) Processed method.

C. The Solution of Single Strip BA Model

Since the equations of the error correction model are nonlinear functions, it must be linearized in order to facilitate leveling calculations and applications. After linearization the error and normal equations can be obtained.

Suppose there are 4 images and 10 numbered object points ($i = 1, 2, 3, 4, 5, 6, 7, 8, 9, 10$), these 10 object points are projected on these 4 images with a total of 26 image points. Of these, six object points, numbered 1, 2, 4, 6, 8, and 9, were imaged on the first image. Six object points, numbered 1, 3, 5, 6, 7, and 10, were imaged on the second image. Seven object points, numbered 1, 2, 5, 6, 8, 9, and 10, were imaged on the third image. Seven object points, numbered 2, 3, 4, 5, 6, 7, and 8, were imaged on the fourth image. Linearization of the collinearity equations formed by each image point can form the error equation, whose expression is shown in

$$\underset{2\times1}{V} = \underset{2\times18}{A}\ \underset{18\times1}{X} - \underset{2\times1}{L}, P \tag{4}$$

where V represents the residual vector of all observed values, and $X = [X_0 \quad X_1 \quad X_2 \quad \ldots \quad \text{roll}_0 \quad \text{roll}_1 \quad \text{roll}_2]^T$ denotes the matrix of unknowns correction value. $A = \begin{bmatrix} a_{1-1} & a_{1-2} & a_{1-3} & \ldots & a_{1-16} & a_{1-17} & a_{1-18} \\ a_{2-1} & a_{2-2} & a_{2-3} & \ldots & a_{2-16} & a_{2-17} & a_{2-18} \end{bmatrix}^T$ denotes the coefficient matrix of parameters (matrix of partial derivatives of parameters). $L = [x_{\text{img}pt} \quad y_{\text{img}pt}]^T$ denotes the matrix of observations. P denotes the weight matrix (2×2) of the image point. All the error equations form a system of error equations, whose coefficient matrix is shown in Fig. 3, where (a) represents the coefficient matrix of the error equation of the traditional aerial triangulation method, and (b) represents the coefficient matrix of the error equation of the proposed method in this article.

Combined with the principle of least squares, the normal equation can then be obtained, and its coefficient matrix structure is shown in Fig. 4, where (a) represents the coefficient matrix structure of the normal equation of the traditional aerial triangulation method and (b) represents the coefficient matrix structure of the normal equation of the method proposed in this article.

As can be seen from Fig. 4, there are m images and n object points, the dimension of the coefficient matrix in normal equation of traditional BA method is $(6m + 3n) \times (6m + 3n)$. The dimension of the coefficient matrix is related to both the number of images and the number of object points. The normal equation coefficient matrix for the method proposed in this article is $(18 + 3n) \times (18 + 3n)$, and its dimension of the coefficient matrix is related to the number of object points only. Therefore, the dimension of matrix decreases of the method in this article is reduced and the computational efficiency is improved.

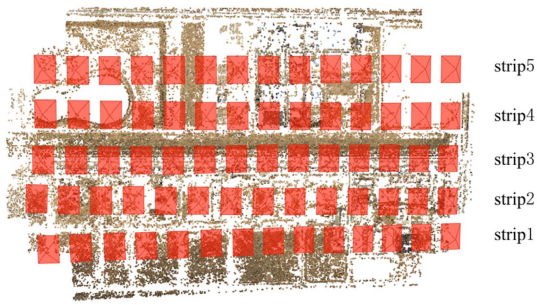

Fig. 5. Schematic diagram of Inner Mongolia Desert experimental survey area.

IV. Experimental Results and Analysis

A. Description of Experimental Data

In order to verify the accuracy and reliability of the method proposed in this article, the experiment is verified with data collected from two experimental areas. These two areas are: the desert region of Inner Mongolia and the campus of Shandong University of Science and Technology. The experiment mainly used three traditional methods to compare the accuracy of proposed method. The three methods are: GPS/IMU direct geographic orientation method (method I), relative and absolute orientation method (method II), and POS assisted BA (method III). The following are overviews of the experimental areas and the detailed parameters of them are given in Table I.

1) *Desert Region of Inner Mongolia*: The experimental area is shown in Fig. 5. This region contains multiple flight strips, but the focus of this article is on a single flight strip. Therefore, five comparative experiments were conducted

TABLE I
DETAILS PARAMETERS OF THE TWO EXPERIMENTAL AREA

Name	Inner Mongolia Area					Campus
Strip id	Strip1	Strip2	Strip3	Strip4	Strip5	Strip
Number of images	14	14	14	14	14	26
Number of CPs	12	12	6	10	10	16
Camera model	IQ180					ILCE5100
Focal length (pixel)	9952.5					6464.7
Image resolution (pixel)	10328×7760					6000×4000
pixel size(mm)	0.0052					0.0054
IMU Accuracy (°)	Horizontal angle		0.01			--
	Heading angle		0.02			--
Airborne RTK Accuracy(m)	Plane 0.02; Height 0.05					Plane 0.02; Height 0.05

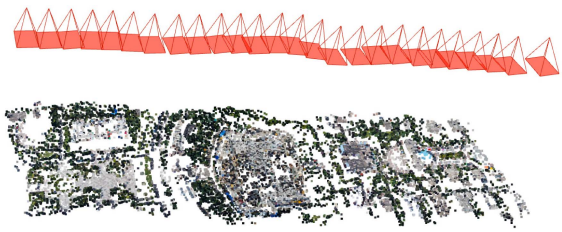

Fig. 6. Schematic diagram of Shandong University of Science and Technology experimental survey area.

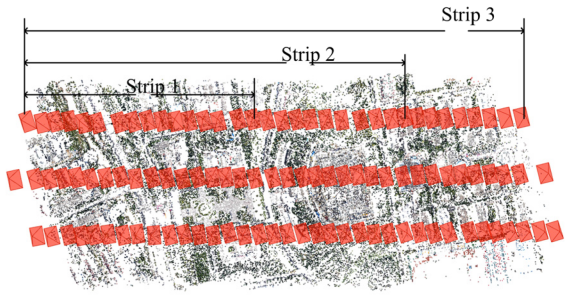

Fig. 7. Schematic diagrams of different lengths of the same flight strip.

on five flight strips. Each flight strip consists of 14 images, in which flight strip 1 providing 12 checkpoints (CPs); strip 2 providing 12 CPs; strip 3 providing 6 CPs; strip 4 providing 10 CPs; and strip 5 providing 10 CPs.

2) *Shandong University of Science and Technology*: The experimental area is shown in Fig. 6. The coverage area contains one flight strip with 26 images, and provides 16 CPs. The coordinates of all CPs in this experiment were obtained through field measurements using real-time kinematic (RTK) techniques with the WGS84 coordinate system.
3) The experimental data for various lengths of the same flight strip in the Shandong University of Science and Technology experimental area is presented in this group of experiments. Three long flight strips, namely strip I, strip II, and strip III, were selected. For each strip, three different lengths were chosen: strip 1 comprised 16 images; strip 2 comprised 26 images; and strip 3 comprised 36 images. The data for this set of experiments is illustrated in Fig. 7.

B. Initial Values and Weights of Model Parameters

The accuracy of the initial values of the parameters in the error correction model will directly affect the accuracy of the final solution. To determine the initial values of the parameters with high accuracy plays a crucial role in the effectiveness of the method in this article. This article adopts the principle of least squares fitting to determine the initial value of the parameters in the error correction model. The difference between the image EO obtained by POS and initial image EO is first calculated, as shown in (5). Then, combining (5) and (1) with at least 3 images, an initial value of 18 parameters can be fitted by least squares. In (5), X_{pos}, Y_{pos}, Z_{pos}, yaw_{pos}, $\text{pitch}_{\text{pos}}$, and roll_{pos} denote the image EO observed by POS data

$$\begin{aligned} X_{\text{pos}} - X_{\text{rel}} &= \Delta X_t \\ Y_{\text{pos}} - Y_{\text{rel}} &= \Delta Y_t \\ Z_{\text{pos}} - Z_{\text{rel}} &= \Delta Z_t \\ \text{yaw}_{\text{pos}} - \text{yaw}_{\text{rel}} &= \Delta \text{yaw}_t \\ \text{pitch}_{\text{pos}} - \text{pitch}_{\text{rel}} &= \Delta \text{pitch}_t \\ \text{roll}_{\text{pos}} - \text{roll}_{\text{rel}} &= \Delta \text{roll}_t. \end{aligned} \tag{5}$$

The fitting effect of the initial values is shown in Fig. 8. The left graph represents the image EO difference between the POS and the initial image EO. The right graph represents the corrected value of the image EO fitted by the error correction model proposed in this article. It can be seen that the overall direction in these two graphs is consistent, which indicates that the error correction model proposed in this article has practical significance.

In traditional BA, the design of the weights for the observations and parameters will directly affect the quality of the results. Therefore, appropriate weights need to be given to different variables to obtain more accurate solution results. While in

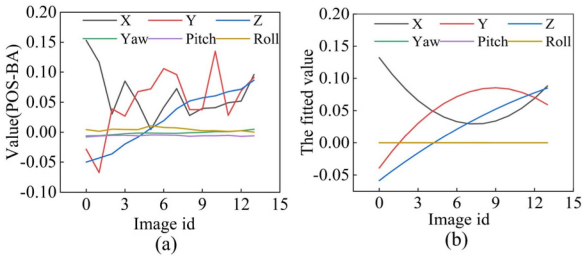

Fig. 8. Diagram of error correction model parameters. fitting effect. (a) Actual value. (b) Fitted value.

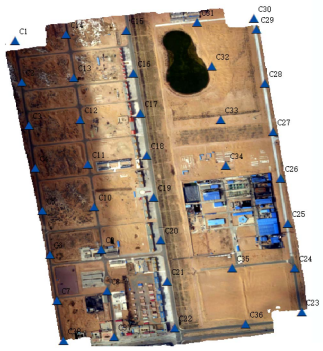

Fig. 9. Layout diagram of CPs in the Inner Mongolia Desert survey area.

TABLE II
OVERALL ACCURACY IMPROVEMENT RATIO OF PROPOSED METHOD COMPARED TO TWO TRADITIONAL METHODS

	Strip 1	Strip 2	Strip 3	Strip 4	Strip 5
Method II	30.65%	13.17%	27.60%	17.58%	35.74%
Method III	24.11%	7.89%	3.50%	4.40%	26.22%

the process of solving the parameters using the collinearity equations, due to the large yaw angle error in the POS data, the method proposed in this article needs to give different weights to the image EO. The yaw angle weight involved in the calculation is smaller than the other parameters, which can minimize the impact due to the yaw angle error.

By multiplying the N_{11} part of the upper left corner of the coefficient matrix in Fig. 4(b) by a diagonal weight matrix. It is equivalent to adding a weight coefficient directly to the diagonal of coefficient matrix. This not only greatly reduces the workload, but also has a design that utilizes the weights of each parameter in the normal equation. This also ensures the positive definiteness of the normal equation coefficient matrix and the stability of the solution.

C. Results and Analysis in the Area of Inner Mongolia Desert Area

In this experimental area, the layout of the CPs is schematically shown in Fig. 9, and the accuracy of results using different methods are shown in Fig. 10. Table II gives the effect of the accuracy improvement in this method with respect to the other two traditional methods.

As shown in Fig. 10 and Table II, the following conclusions can be derived. Method I, due to the influence of position and attitude error in POS data, the accuracy of this method's results does not meet the needs of practical applications. While the attitude angle data of method II is obtained by relative orientation, and its accuracy is improved compared with the method I. POS assisted BA is currently the mainstream method for solving aerial triangulation process and offers the best solution accuracy among the three traditional methods. It is concluded that the POS assisted single strip BA model proposed in this article has a higher solution accuracy than the other three traditional methods when no GCP is involved. The proposed method improves 13.17%-35.74% compared with method II, and improves 3.50%-26.22% compared with method III.

On average, in terms of planimetric accuracy, as shown in Fig. 10(a). The proposed method improves 33.92% compared with method II and 12.9% compared with method III. And in terms of elevation accuracy, as shown in Fig. 10(b). The proposed method has different degrees of improvement compared with Method II and Method III, which are 22.59% and 14.14%, respectively.

D Results and Analysis in the Area of Shandong University of Science and Technology

In the experimental area of Shandong University of Science and Technology, there are 16 CPs, and the layout of CPs in the area is shown in Fig. 11. In order to verify the effect of proposed method compared with other methods in different accuracy of attitude angle cases, this experiment adds different ranges of Gaussian errors to the POS data. Table III and Fig. 12 show the image EO accuracy results obtained by the four methods after adding different Gaussian errors.

Combining the results of four groups of data with different attitude angle errors added in Table III and Fig. 11. It can be concluded that the method proposed in this article improves 2.31%, 21.49%, 32.42%, and 14.66%, respectively, compared with method III. Among them, the improvement of the first group with the proposed method is not good. This is because the data used in the first group of experiments is the original EO of the image and no error is introduced. The later three groups of experiments can be seen that, within a certain error range, the larger the error of attitude angle addition, the more significant the improvement effect of the proposed method is. However, it should be noted that in the fourth group of experiments, the improvement effect of proposed method is slightly decreased compared with the former two groups of experiments. This is because the introduced attitude angle error in this group of experiments is too large, resulting in poor initial accuracy of EO parameters in BA. Consequently, the proposed method cannot fully eliminate the impact of cumulative errors in this scenario.

Fig. 13 depicts the effect of comparing the flight strip model obtained using method II and the proposed method with the flight strip model obtained from the original POS data. In this figure, the blue line indicates the flight strip model obtained by method II, the red line indicates the flight strip model obtained by the proposed method, and the black line indicates the flight

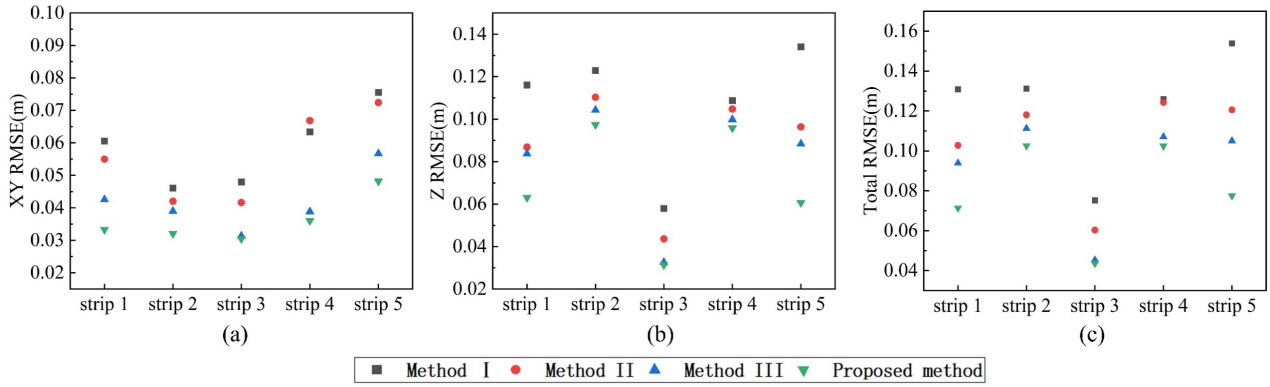

Fig. 10. Analysis of Experimental Accuracy in the Inner Mongolia Desert Region. GPS/IMU direct geographic orientation method (Method I), relative and absolute orientation method (Method II), and POS assisted BA (Method III).

TABLE III
ANALYSIS OF EXPERIMENTAL ACCURACY IN SHANDONG UNIVERSITY OF SCIENCE AND TECHNOLOGY

	Method	XY RMSE(m)	Z RMSE(m)	Total RMSE(m)
Data 1: No add error	Method I	0.099	0.189	0.204
	Method II	0.171	0.255	0.307
	Method III	0.109	0.134	0.173
	Proposed method	0.078	0.137	0.169
Data 2: 0.001°-0.01°	Method I	0.328	0.200	0.384
	Method II	0.191	0.211	0.284
	Method III	0.275	0.166	0.321
	Proposed method	0.201	0.152	0.252
Data 3: 0.01°-0.1°	Method I	0.605	1.412	1.537
	Method II	0.460	0.231	0.515
	Method III	0.395	0.397	0.560
	Proposed method	0.342	0.193	0.393
Data 4: 0.1°-0.5°	Method I	2.206	5.105	5.561
	Method II	1.682	2.548	3.054
	Method III	1.499	1.442	2.080
	Proposed method	1.112	1.383	1.775

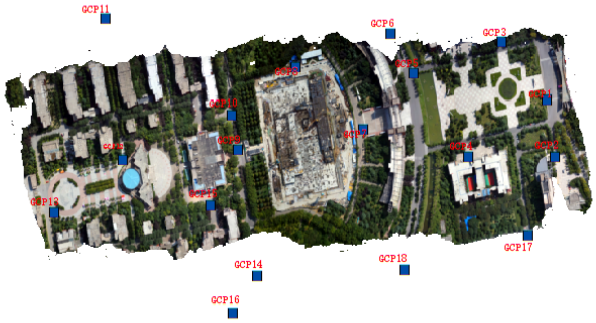

Fig. 11. Layout diagram of CPs in Shandong University of Science and Technology.

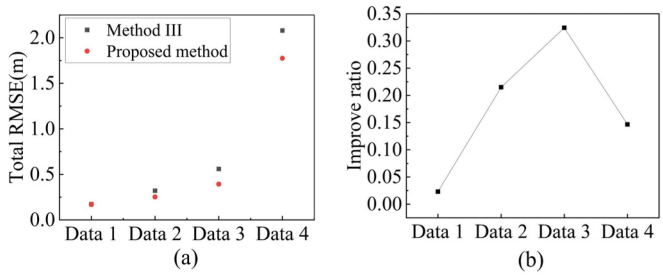

Fig. 12. Comparison of the results of the two methods at different accuracy attitude angles. (a) Total RMSE. (b) Improve ratio.

strip model observed by POS. It can be seen from this figure that the flight strip model after relative orientation has a large deformation comparing the POS data. Through the improvement by proposed method, the position of the obtained flight strip model is closer to the POS data. It indicates that the proposed method successfully eliminates the effect of cumulative error, making the position of the flight strip closer to the real situation. In addition, the shape of the flight strip model obtained by the proposed method is closer to that obtained by method II. It indicates that the proposed method retains the accurate relative position relationship in method II. In summary, the proposed method can eliminate the influence of the accumulated errors of method II on the flight strip model without losing the relative position relationship.

E. Results and Analysis of the Same Flight Strip With Different Lengths

In order to verify the effectiveness of this article method in improving the bending of the flight strip under different image

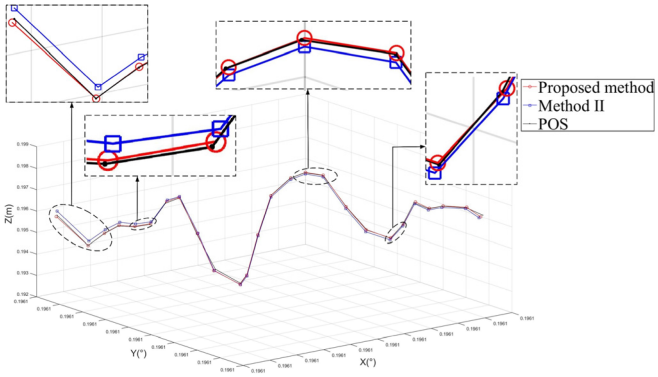

Fig. 13. Comparison of the strip models obtained using the two methods.

TABLE IV
ANALYSIS OF EXPERIMENTAL ACCURACY IN THE CASE OF DIFFERENT LENGTHS OF THE SAME FLIGHT STRIP

		Method	Total RMSE (m)
Strip I	Strip 1	Method II	0.938
		Proposed method	0.657
	Strip 2	Method II	0.329
		Proposed method	0.211
	Strip 3	Method II	0.501
		Proposed method	0.303
Strip II	Strip 1	Method II	0.229
		Proposed method	0.138
	Strip 2	Method II	0.307
		Proposed method	0.169
	Strip 3	Method II	0.605
		Proposed method	0.337
Strip III	Strip 1	Method II	0.553
		Proposed method	0.480
	Strip 2	Method II	0.505
		Proposed method	0.415
	Strip 3	Method II	0.576
		Proposed method	0.364

TABLE V
PERCENTAGE OF ENHANCEMENT IN THIS ARTICLE METHOD COMPARED TO METHOD II

	Strip 1	Strip 2	Strip 3
Strip I	29.89%	35.79%	39.35%
Strip II	39.6%	44.89%	44.25%
Strip III	13.26%	17.71%	36.64%

numbers. In this experiment, three sub-strips with different numbers of images are intercepted in the same flight strip, and three different flight strips are selected to repeat the experiment. The results of the experiment are shown in Table IV and Fig. 14. Table V and Fig. 15 depict the improvement in flight strip bending achieved by the proposed method compared to Method II, considering various lengths of the same flight strip.

Table V and Fig. 16 illustrate that as the flight strip length varies, the proposed method shows increasingly enhanced accuracy compared to method II, particularly evident with longer flight strips. As the flight strip length expands from 16 to 26 and 36, when compared to method II, the improvement ratio in experimental accuracy for the proposed method escalates from 29.89% to 35.79% and 39.35% in Strip I. For strip III, the experimental accuracy improvement ratio of proposed method over method II increases from 13.26% to 17.71% and 36.64%. The bending of the flight strip results from error accumulation during the model construction in relative orientation. It can be concluded that the method proposed in this article effectively mitigates error accumulation, addressing the issue of flight strip bending. Moreover, the improvement becomes more obvious with longer flight strips. Among them, in strip II, the experimental accuracy improvement ratio of proposed method over method II increases from 39.6% to 44.89% and 44.25%. In this strip, the improvement ratio has a decreasing trend, which is caused by the uneven distribution of CPs in this strip, and this decreasing trend is within the normal range.

Fig. 15 is a schematic diagram of the flight strip model constructed by the method of this article with method II and method III. In Fig. 15(a), there are only 16 images in this flight strip. From the last section of the flight strip, it be seen that the flight strip model obtained by proposed method is closer to the flight strip model obtained by method III compared to method II, but it is very insignificant. In Fig. 15(b) and (c), the number of images in the flight strip increases from 16 to 26 and 36. This demonstrates that the flight strip model obtained through the proposed method closely aligns with method III, and the trend of convergence becomes increasingly evident. This validates the effectiveness of the proposed method in addressing flight strip bending, especially in cases of longer flight strip lengths.

V. DISCUSSION

This article innovatively proposed a POS assisted aerial triangulation method for single flight strip without GCPs. This method effectively eliminates the influence of error accumulation on the flight strip by relative orientation method, and solved the problem of the flight strip deformation. The main contribution of this article lies in the combination of the advantages of relative method and traditional aerial triangulation. As a result, this article will be able to obtain a high-quality flight strip model that is not affected by the accumulation of errors in the relative orientation methods. In addition, the number of unknowns in the solution process is independent in the number of images, which greatly improves the computational efficiency.

This method has the following limitations. It relies on the accuracy of POS data, and when the accuracy of POS data is low, the improvement effect of the method is not significant. In addition, the improvement effect of the method in this article will be more obvious in the case of long flight strip, but due to the limited data conditions, the longest only 36 images are used in the experiments of this article.

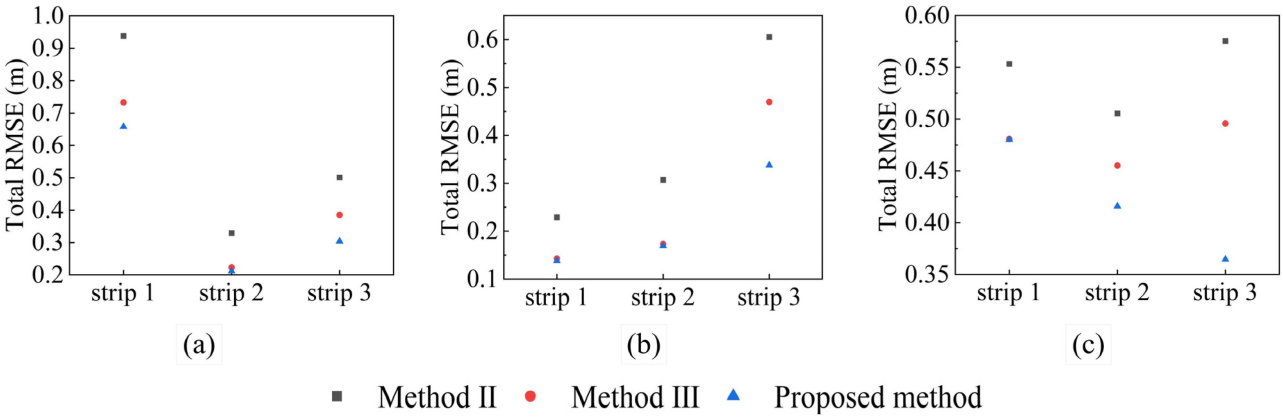

Fig. 14. Accuracy under different methods for three flight strips. (a) Strip I. (b) Strip II. (c) Strip III.

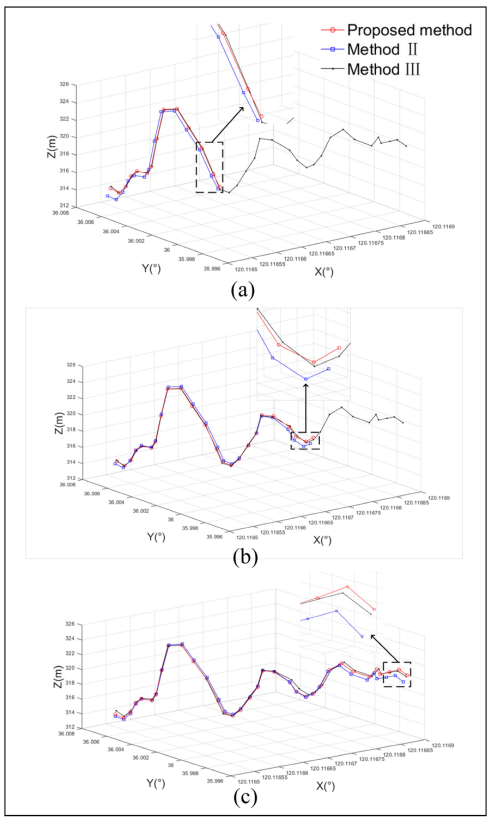

Fig. 15. Visualization of the effect of this article method to improve the bending effect of the flight strip. (a) Strip 1. (b) Strip 2. (c) Strip 3.

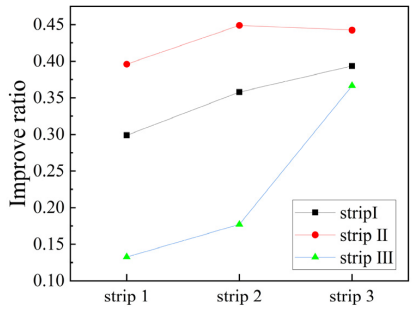

Fig. 16. Line graph of the improvement effect of this method compared to method II.

VI. Conclusion

While traditional POS assisted single strip aerial triangulation methods have addressed the reliance on GCPs, they have not considered the issue of error accumulation during the construction of relative orientation models. Therefore, this article proposes a method of POS assisted single strip aerial triangulation taking into account the cumulative error of relative orientation to solve the problem. The method fully considers the effect of relative orientation accumulation error and introduces it into the BA model for solving. The solving accuracy is further improved based on traditional POS assisted BA. In two regions, Inner ·Mongolia Desert Region and Shandong University of Science and Technology, three different traditional methods were selected to experimentally compare and comprehensively analyze with the proposed method. The conclusions reached are shown as follows.

1) In the desert region of Inner Mongolia, the five flight strips in the region were experimented separately. The final experiment can show that the accuracy of proposed method is improved by 24.95% on average compared with the relative orientation and absolute orientation method and by 13.22% on average compared with the POS assisted BA.
2) In the area of Shandong University of Science and Technology, when the attitude angle is increased to a small interval of (0.001–0.1) error, with the gradual increase of the error, the method of this article compared to the POS assisted BA gradually increases the degree of enhancement, from the enhancement of 21.49% to enhancement of 32.42%. However, when the angle of the attitude add the error is too large (0.1–0.5), the proposed method compared to the POS assisted BA only improves 14.66%.
3) In the third set of experiments, this article can clearly conclude that when there are more than three images in the flight strip, the more images in the strip, i.e., the longer the flight strip, the more obvious the effect of the proposed method to improve the bending phenomenon of the flight strip.

As a result of the above experiments, the solution accuracy of proposed method outperforms that of the relative and absolute orientation method and the POS assisted BA method. And when the length of the flight strip is longer, the proposed method solves the flight strip bending more effectively compared with other traditional methods. This is particularly notable in the case of emergency mapping, mobile surveying and special terrain such as narrow and long zones without GCPs single strip. It achieves the expected experimental effect and is of practical significance for the production of photogrammetric data from unmanned aerial vehicles.

REFERENCES

[1] F. He and A. Habib, "Automated relative orientation of UAV-based imagery in the presence of prior information for the flight trajectory," *Photogramm. Eng. Remote Sens.*, vol. 82, no. 11, pp. 879–891, 2016.

[2] A. Gregorini, N. Cattaneo, S. Bortolotto, S. Massa, M. F. Bocciolone, and E. Zappa, "Metrological issues in 3D reconstruction of an archaeological site with aerial photogrammetry," in *Proc. IEEE Int. Instrum. Meas. Technol. Conf.*, 2023, pp. 1–6.

[3] M. Lemmens, "A survey on stereo matching techniques," *Int. Arch. Photogramm. Remote Sens.*, vol. 27, pp. 11–23, Jan. 1988.

[4] H. Stewénius, C. Engels, and D. Nistér, "Recent developments on direct relative orientation," *ISPRS J. Photogramm. Remote Sens.*, vol. 60, no. 4, pp. 284–294, 2006.

[5] Y. Zhang, B. - H. Hu, and J. Zhang, "Relative orientation based on multi-features," *ISPRS J. Photogramm. Remote Sens.*, vol. 66, no. 5, pp. 700–707, 2011.

[6] T. Läbe, "Automatic relative orientation of images," *Photogramm. Eng. Remote Sens.*, vol. 62, no. 1, pp. 47–55, 2006.

[7] H. Zhao et al., "Aerial photography flight quality assessment with GPS/INS and DEM data," *ISPRS J. Photogramm. Remote Sens.*, vol. 135, pp. 60–73, 2018.

[8] C. Fraser, M. Ravanbakhsh, and M. Awrangjeb, "Precise georeferencing in the absence of ground control: A strip adjustment approach," *Int. Arch. Photogramm., Remote Sens. Spatial Inf. Sci.*, vol. 31, pp. 1–4, 2009.

[9] J. Shi, X. Yuan, Y. Cai, and G. Wang, "GPS real-time precise point positioning for aerial triangulation," *GPS Solutions*, vol. 21, no. 2, pp. 405–414, 2017.

[10] K. El-Ashmawy, "Photogrammetric block adjustment without control points," *Geodesy Cartogr.*, vol. 44, pp. 6–13, Apr. 2018.

[11] J. Liu, W. Xu, B. Guo, G. Zhou, and H. Zhu, "Accurate mapping method for UAV photogrammetry without ground control points in the map projection frame," *IEEE Trans. Geosci. Remote Sens.*, vol. 59, no. 11, pp. 9673–9681, Nov. 2021, doi: 10.1109/TGRS.2021.3052466.

[12] E. Sanz-Ablanedo, J. H. Chandler, J. R. Rodríguez-Pérez, and C. Ordóñez, "Accuracy of unmanned aerial vehicle (UAV) and SfM photogrammetry survey as a function of the number and location of ground control points used," *Remote Sens.*, vol. 10, no. 10, 2018, Art. no. 1606.

[13] S. B. Hong, C. M. Kang, S. - H. Lee, and C. C. Chung, "Multi-rate vehicle side slip angle estimation using low-cost GPS/IMU," in *Proc. 17th Int. Conf. Control, Automat. Syst.*, 2017, pp. 35–40.

[14] J. Liu, W. Huang, and B. Guo, "Conjugated-point positioning method based on multiview images," *IEEE Trans. Geosci. Remote Sens.*, vol. 61, Feb. 2023, Art. no. 5604611, doi: 10.1109/TGRS.2023.3247919.

[15] J. - C. Padró, F. - J. Muñoz, J. Planas, and X. Pons, "Comparison of four UAV georeferencing methods for environmental monitoring purposes focusing on the combined use with airborne and satellite remote sensing platforms," *Int. J. Appl. Earth Observ. Geoinf.*, vol. 75, pp. 130–140, Mar. 2019,.

[16] J. Liu and W. Guo, "Multi-platform bundle adjustment method supported by object structural information," *IEEE J. Sel. Topics Appl. Earth Observ. Remote Sens.*, vol. 17, pp. 1204–1214, Oct. 2024, doi: 10.1109/JSTARS.2023.3339293.

[17] Y. Zhang, B. - H. Hu, and J. Zhang, "Relative orientation based on multi-features," *ISPRS J. Photogramm. Remote Sens.*, vol. 66, pp. 700–707, 2011.

[18] H. C. Longuet-Higgins, "A computer algorithm for reconstructing a scene from two projections," *Nature*, vol. 293, no. 5828, pp. 133–135, Sep. 1981.

[19] D. Nister, "An efficient solution to the five-point relative pose problem," *IEEE Trans. Pattern Anal. Mach. Intell.*, vol. 26, no. 6, pp. 756–770, Jun. 2004, doi: 10.1109/TPAMI.2004.17.

[20] L. Kneip and S. Lynen, "Direct optimization of frame-to-frame rotation," in *Proc. IEEE Int. Conf. Comput. Vis.*, 2013, pp. 2352–2359.

[21] L. Kneip, R. Siegwart, and M. Pollefeys, "Finding the exact rotation between two images independently of the translation," in *Proc. Eur. Conf. Comput. Vis.*, 2012, pp. 696–709.

[22] A. W. Habib and D. Kelley, "Automatic relative orientation of large scale imagery over urban areas using modified iterated hough transform," *ISPRS J. Photogramm. Remote Sens.*, vol. 56, no. 1, pp. 29–41, 2001.

[23] F. He, T. Zhou, W. Xiong, S. M. Hasheminnasab, and A. W. Habib, "Automated aerial triangulation for UAV-based mapping," *Remote. Sens.*, vol. 10, no. 12, 2018, Art. no. 1952.

[24] D. Turner, A. Lucieer, and L. Wallace, "Direct georeferencing of ultrahigh-resolution UAV imagery," *IEEE Trans. Geosci. Remote Sens.*, vol. 52, no. 5, pp. 2738–2745, May 2014, doi: 10.1109/TGRS.2013.2265295.

[25] S. Tanathong and I. Lee, "Using GPS/INS data to enhance image matching for real-time aerial triangulation," *Comput. Geosci.*, vol. 72, pp. 244–254, Nov. 2014.

[26] D. Wierzbicki, "Determination of shift/bias in digital aerial triangulation of UAV imagery sequences," *IOP Conf. Ser., Earth Environ. Sci.*, vol. 95, no. 3, pp. 032–033, Dec. 2017.

[27] K. Choi and I. Lee, "A sequential aerial triangulation algorithm for real-time georeferencing of image sequences acquired by an airborne multi-sensor system," *Remote Sens.*, vol. 5, no. 1, pp. 57–82, 2013. [Online]. Available: https://www.mdpi.com/2072-4292/5/1/57

[28] G. Forlani, L. Pinto, R. Roncella, and D. Pagliari, "Terrestrial photogrammetry without ground control points," *Earth Sci. Inform.*, vol. 7, no. 2, pp. 71–81, Jun. 2014.

[29] C. S. Fraser, M. Ravanbakhsh, and M. Awrangjeb, "Precise georeferencing in the absence of ground control: A strip adjustment approach," 2009.

Jianchen Liu was born in Jiamusi, Heilongjiang, China, in 1987. He received the M.S. degree in geomatics engineering from the Shandong University of Science and Technology, Qingdao, China, in 2013, and the Ph.D. degree in photogrammetry and remote sensing from the School of Remote Sensing and Information Engineering, Wuhan University, Wuhan, China, in 2017.

He is currently an Associate Professor with the College of Geodesy and Geomatics, Shandong University of Science and Technology. His research interests include UAV photogrammetry, computer stereovision, and 3-D modeling by oblique images.

Rumeng Li was born in Weifang, Shandong, China, in 1998. She received the B.S. degree in geomatics engineering from the Shandong Jianzhu University, Jinan, China, in 2021. She is currently working toward the master's degree in digital photogrammetry with Shandong University of Science and Technology, Qingdao, China.

Wei Guo was born in Heze, Shandong, China, in 1999. He received the B.S. degree in geomatics engineering in 2021 from the Shandong University of Science and Technology, Qingdao, China, where he is currently working toward the master's degree in digital photogrammetry.